

# Effects of Side-Chain Interdigitation on Stability: An Environmentally, Electrically, and Thermally Stable Semiconducting Polymer

Danbi Choi,<sup>†</sup> Ban-Seok Jeong,<sup>‡</sup> Byungcheol Ahn,<sup>§</sup> Dae Sung Chung,<sup>†</sup> Kimin Lim,<sup>‡</sup> Se Hyun Kim,<sup>†</sup> Seon Uk Park,<sup>†</sup> Moonhor Ree,<sup>\*,§</sup> Jaejung Ko,<sup>\*,‡</sup> and Chan Eon Park<sup>\*,†</sup>

<sup>†</sup>POSTECH Organic Electronics Lab, Polymer Research Institute, Department of Chemical Engineering, Pohang University of Science and Technology, Pohang 790-784, Korea

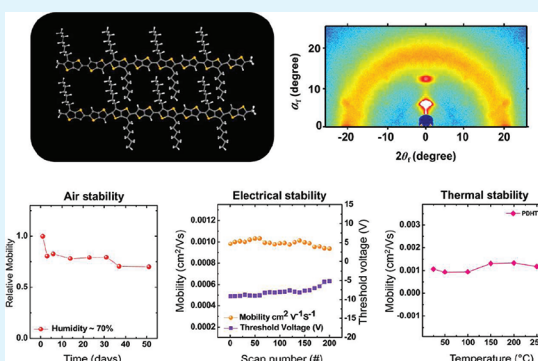
<sup>‡</sup>Department of New Materials Chemistry, Korea University Jochiwon, Chungnam 339-700, Korea

<sup>§</sup>Department of Chemistry, Pohang Accelerator Laboratory, Center for Electro-Photo Behaviors in Advanced Molecular Systems, Division of Advanced Materials Science, Polymer Research Institute, and BK School of Molecular Science, and Pohang University of Science and Technology, Pohang, 790-794, Korea

## Supporting Information

**ABSTRACT:** A polymeric semiconductor, poly(3,6-dihexyl-[2,2']bi[thieno[3,2-b]thiophene]) (PDHTT), was synthesized and tested as an active layer in organic thin film transistors (OTFTs). This semiconductor showed considerable potential for use in commercial electronic devices because of its superior characteristics, particularly its good stability. PDHTT-based OTFTs exhibited high stability in air, retaining their initial performance after exposure to 70% relative humidity for 50 days; they were also stable under repeated electrical stress and even after exposure to temperatures as high as 250 °C. We attribute the remarkable stability of PDHTT OTFTs to the relatively low highest occupied molecular orbital (5.1 eV) level of the polymer and its highly interdigitated structure in the thin film state.

**KEYWORDS:** poly(3,6-dihexyl-[2,2']bi[thieno[3,2-b]thiophene]) (PDHTT), air stability, electrical stability, thermal stability



## INTRODUCTION

Polymeric organic semiconductors (OSCs) with high field-effect mobility ( $\mu$ ) have been intensively developed and studied for use as active layers in organic electronics.<sup>1–3</sup> However, OSCs are easily oxidized and degrade under air, repeated electrical stress, and at high temperatures; these problems must be overcome before devices based on OSCs can become commercially viable.<sup>4</sup>

Some semiconductors have been developed that are less susceptible to oxidation and thus have greater stability in air than conventional thiophene-based polymers.<sup>5–7</sup> However, the successful commercialization of OSCs requires stable device operation under repeated electrical stress and at high temperatures. Unfortunately, the transfer curves of many OSCs shift after repetitive sweeps, and the active layers are degraded by high temperatures.<sup>8,9</sup>

This article assesses the usefulness of poly(3,6-dihexyl-[2,2']bi[thieno[3,2-b]thiophene]) (PDHTT) as a semiconductor layer for use in organic thin film transistors (OFETs). PDHTT was designed to have the following features: (1) a fused aromatic ring to provide a rigid backbone structure, and (2) a hexyl side chain on the backbone. A rigid backbone provides thermal stability, and the fused aromatic ring enables the charges to be delocalized along the backbone, which reduces the highest occupied molecular orbital (HOMO) level

and thereby increases resistance to oxidation. The hexyl side chain facilitates interdigitation between adjacent polymer chains. Interdigitation improves interlayer stacking by resulting in a three-dimensional crystalline structure,<sup>10</sup> which in turn improves the electrical or thermal stability, or both, by increasing the packing density and decreasing the number of defects. As a result, PDHTT has remarkable resistance to oxidation in air (air stability), exhibits consistent  $\mu$  under repeated electrical stress (electrical stability), and resists breakdown at high temperatures (thermal stability), which have not previously been observed together in a single polymer.

## EXPERIMENTAL SECTION

**Synthesis.** Thieno[3,2-b]thiophene (1) and 2,5-dibromo-3,6-dihexylthieno[3,2-b]thiophene (4) were synthesized according to the procedure reported in the literature.<sup>11,12</sup> <sup>1</sup>H nuclear magnetic resonance (<sup>1</sup>H NMR) spectra were recorded with a Varian Mercury 300 spectrometer.

2,5-Dibromothieno[3,2-b]thiophene (2):<sup>19</sup> thieno[3,2-b]thiophene (1.5 g, 17.0 mmol) was dissolved in DMF (40 mL) and cooled to 0 °C. In the dark, the solution was slowly added to N-bromosuccinimide

Received: September 23, 2011

Accepted: December 23, 2011

Published: December 23, 2011

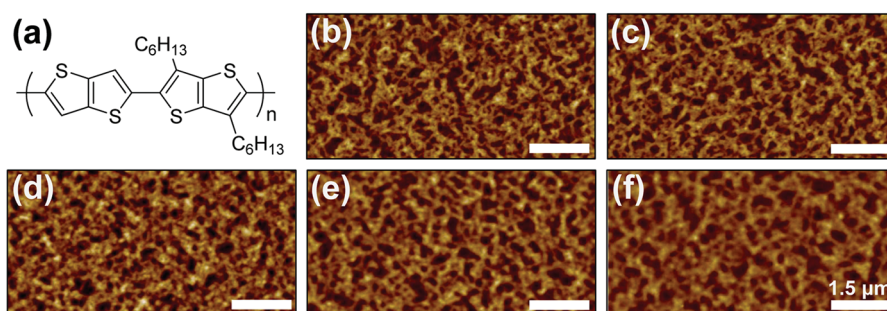


**Figure 1.** (a) Chemical structure of PDHTT. AFM images of (b) an unannealed PDHTT film (as-spun), and PDHTT films annealed at (c) 100 °C, (d) 150 °C, (e) 200 °C, and (f) 250 °C.

(3.808 g, 34.0 mmol) in small portions. After stirring for 3 h with cooling in an ice bath, the solution was extracted with  $\text{CH}_2\text{Cl}_2$  and washed with water. The extracts were dried over  $\text{MgSO}_4$  and concentrated under reduced pressure. The residue was purified by silica column chromatography using hexane as an eluent to yield a white solid (93%). This compound was unstable and decomposed easily.  $^1\text{H}$  NMR ( $\text{CDCl}_3$ , 300 MHz, ppm):  $\delta$  7.18 (s, 2H).

**2,5-Bis(trimethylstannyl)thieno[3,2-b]thiophene (3):** 2,5-dibromothieno[3,2-b]thiophene (**2**) (3.00 g, 10 mmol) was dissolved in anhydrous  $\text{Et}_2\text{O}$  (200 mL) and cooled to 0 °C under a nitrogen atmosphere. A solution of *n*-butyllithium (15 mL of a 1.6 M solution in hexane, 24 mmol) was added dropwise. After stirring at 0 °C for 10 min, a solution of  $\text{Me}_3\text{SnCl}$  (23 mL 1.0 M solution in tetrahydrofuran (THF), 23 mmol) was added to the solution, followed by stirring for 2 h. The reaction was quenched by the addition of water, extracted with  $\text{Et}_2\text{O}$ , dried over  $\text{MgSO}_4$ , and concentrated under reduced pressure. The resulting mixture was dissolved in  $\text{Et}_2\text{O}$  and treated with activated carbon. Then the crude product was filtered through a plug of silica gel eluting with hexane/triethylamine (10:1) and recrystallized from  $\text{EtOH}$  to afford the product as white solid. (66%).  $^1\text{H}$  NMR ( $(\text{CD}_3)_2\text{CO}$ , 300 MHz, ppm):  $\delta$  7.37 (s, 2H), 0.39 (s, 18H).

**Polymerization.** 2,5-Bis(trimethylstannyl)thieno[3,2-b]thiophene (**3**) (0.18 g, 0.39 mmol), 2,5-dibromo-3,6-dihexylthieno[3,2-b]thiophene (**4**) (0.18 g, 0.39 mmol), and  $\text{Pd}(\text{PPh}_3)_4$  (22.3 mg, 0.019 mmol) were dissolved in anhydrous toluene (40 mL) under nitrogen and heated at 130 °C with stirring for 24 h. The reaction mixture was poured into  $\text{MeOH}$  (100 mL), and the resulting precipitate was stirred for 1 h. The solution was filtered and purified by Soxhlet extraction with  $\text{MeOH}$  for 2 days. The polymer was dried to yield polymer (**5**) (89%).  $^1\text{H}$  NMR ( $\text{CDCl}_3$ , 300 MHz, ppm):  $\delta$  7.27 (br s, 2H), 2.94 (br m, 4H), 1.77 (br m, 4H), 1.34 (br m, 12H), 0.90 (br t, 6H) (see the Supporting Information S1).

**Characterization of Structure and Morphology of PDHTT Film.** Grazing incidence X-ray scattering (GIXS) measurements were conducted at the 4C2 beamline in the Pohang Accelerator Laboratory using a monochromatized X-ray radiation source of 8.979 eV ( $\lambda = 0.138$  nm) and a two-dimensional (2D) charge-coupled device (CCD) detector (Roper Scientific, Trenton, NJ, USA). The distance between the sample and the detector was 132.7 mm. The samples were mounted on a homemade *z*-axis goniometer equipped with a vacuum chamber. The incidence angle ( $\alpha_i$ ) of each X-ray beam was set to 0.16°. Scattering angles were determined from the positions of the X-ray beams reflected from the silicon substrate interface as a function of the incident angle  $\alpha_i$  and with respect to scattering from precalibrated silver behenate (TCl, Japan). Data were typically collected for 60 s.

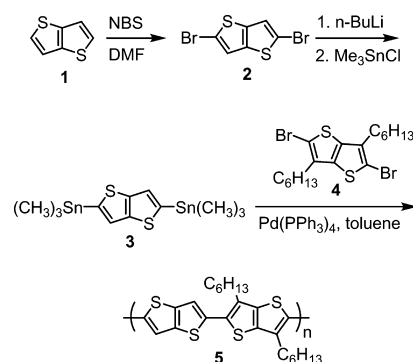
The morphology of the PDHTT film was investigated by Atomic force microscopy (AFM; Digital Instrument Multimode SPM) in tapping mode. The HOMO level was determined from the cyclic voltammetry (vs  $\text{Ag}/\text{AgCl}$ ) and the optical band gap was calculated by UV–vis measurement (Cary 5000, Varian Co.). The side-chain interdigitation was analyzed by Fourier transform infrared (FTIR) spectroscopy (Nicolet 6700, Thermo Elec. Co.). The degradation temperature ( $T_d$ ) of the PDHTT was measured in the range 50–700 °C using a Seiko thermogravimeter (TG/DTA-6300).

**Device Fabrication.** The PDHTT-based OTFTs were fabricated as follows. A heavily doped (100) Si wafer was used as the gate electrode and a thermally grown 300-nm-thick layer of  $\text{SiO}_2$  was used as the gate dielectric. The gate dielectric surface was modified with octyltrichlorosilane to convert the surface from hydrophilic to hydrophobic. A 0.4 wt % solution of PDHTT in 1,2,4-trichlorobenzene was spin-coated at 1500 rpm for 120 s; the resulting film was ~40 nm thick, as confirmed with surface-profiling measurements (Alpha Step 500, Tencor). Gold source and drain electrodes (100 nm) were then defined on top of the semiconductor by using a shadow mask. The electrical characteristics of the PDHTT OTFTs were determined by using Keithley 2400 and 236 source/measure units under ambient conditions.

## RESULTS AND DISCUSSION

PDHTT (Figure 1) was synthesized as described in Scheme 1.<sup>11,12,21–23</sup> Gel permeation chromatography was used to show

### Scheme 1. Synthesis of Poly(3,6-dihexyl-[2,2']bithieno[3,2-b]thiophene) (PDHTT)



that  $M_n$  of the THF-soluble fraction of the polymer is 3.2  $\text{kgmol}^{-1}$ . By using UV–vis spectroscopy and cyclic voltammetry, we found that PDHTT has an optical band gap of 2.06 eV (see the Supporting Information S2a), and a HOMO level of 5.10 eV, which is 0.22 eV lower than the HOMO level of regioregular poly(3-hexylthiophene) (rr-P3HT) (see the Supporting Information S2b) and comparable to those of poly[5,5'-bis(3-dodecyl-2-thienyl)-2,2'-bithiophene] (PQT-12) and poly(2,5-bis(3-alkylthiophen-2-yl)thieno[3,2-b]thiophenes) (PBTTT).<sup>5,6</sup> The value of  $\lambda_{\text{max}}$  (film) of PDHTT was determined to be 460 nm.

The atomic force microscopy (AFM) images in Figure 1b–f shows that the surface morphology of the PDHTT film consists of nanowire-like structures. Roughness of the PDHTT films were in the range of 6.4–6.6 nm. The microstructure of PDHTT film was investigated with grazing incidence X-ray

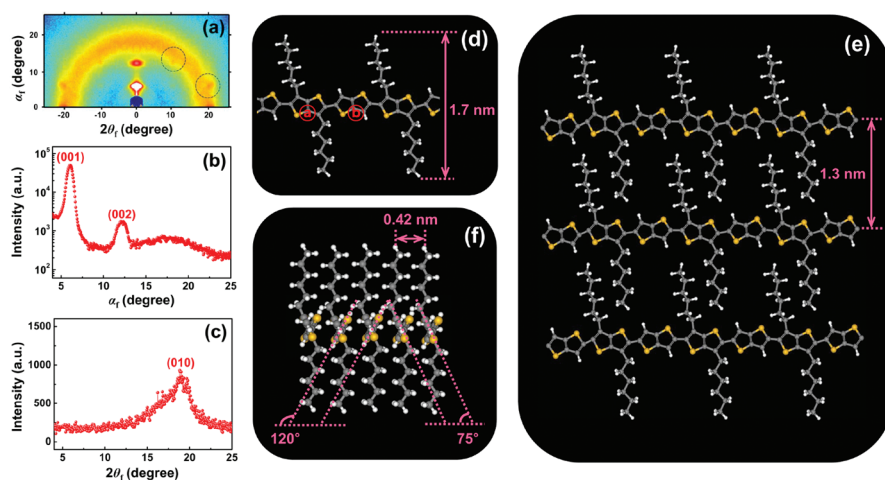


**Figure 2.** (a) 2D GIXS pattern of a PDHTT film. 1D profiles extracted from the 2D GIXS pattern: (b) in the  $\alpha_i$  direction at  $2\theta_i = 0^\circ$  and (c) in the  $2\theta_i$  direction at  $\alpha_i = 0.18^\circ$ . (d) Molecular model of PDHTT. The atoms are colored as follows: C, gray; H, white; S, yellow. Schematic diagrams of the molecular packing in the PDHTT film, showing (e) the interdigitated and (f)  $\pi$ - $\pi$  stacked structures.

scattering (GIXS) (Figure 2a–c). The out-of plane scattering profile of the PDHTT film shows high order peaks from layered structure at  $\alpha_i = 6.06^\circ$  and  $12.2^\circ$  which correspond to the  $d$ -spacing of 1.30 and 0.65 nm, respectively. These peaks indicate first and second order peak of the layered structures of the PDHTT thin film. In addition, the GIXS pattern contains weak, broad isotropic scattering halo around  $19^\circ$ ; the  $d$ -spacing of the halo was estimated to be 0.42 nm, which is probably originated from interdistance between alkyl side chains or  $\pi$ - $\pi$  stacking, or both. Also additional dot patterns in the GIXS are observed due to distorted coplanarity: the two neighboring thienothiophene units (Ⓐ, Ⓑ, Figure 2d) are tilted at angles of  $75$  and  $120^\circ$  with respect to the substrate (Figure 2f), which results in a  $\pi$ - $\pi$  stacking distance of 4.2 Å that is slightly larger than the values of other OSCs.

Using the GIXS results and the molecular simulation analysis (Discovery Studio 2.0 software package), we constructed a molecular model of the PDHTT thin film to estimate chain packing aspects (Figure 2d–f): the dimension of PDHTT molecule with extended side chains was estimated to be  $\sim 1.7$  nm (Figure 2d). The distance of 1.3 nm in the GIXS result (Figure 2e) is a little shorter than the simulation data, which is expected that approximately four methylene units in the alkyl side chains are interdigitated with methylene groups in the side chains of the adjacent PDHTT molecule.<sup>21</sup>

The side-chain interdigitation of the PDHTT was supported by the findings of FTIR and 2D GIXS analyses (Figure 3). The feature in the FTIR spectrum at  $2921.6\text{ cm}^{-1}$  corresponds to the antisymmetric stretch of methylene in the PDHTT, implying a high degree of order and all-trans alkane chains (Figure. 3a).<sup>10</sup> Also, the strong bands at  $1456$  and  $1380\text{ cm}^{-1}$  are attributed to linear methylene groups in the highly crystallized PDHTT film.<sup>24</sup> The 2D GIXS data in Figure 3b show the scattering density along the azimuth angle at  $19^\circ$ . The intensity profile is scanned from  $0^\circ$  (out-of-plane) to  $90^\circ$  (in-plane). If the polymer film contained noninterdigitated and entangled side chains, the intermolecular distances would be similar at all angles, and hence the generated X-ray scattering intensity would be almost equivalent along the azimuth angle. However, the scattering density is significantly increased at  $90^\circ$ , indicating the regular alignment of side chains; these findings strongly indicate side-chain interdigitation.

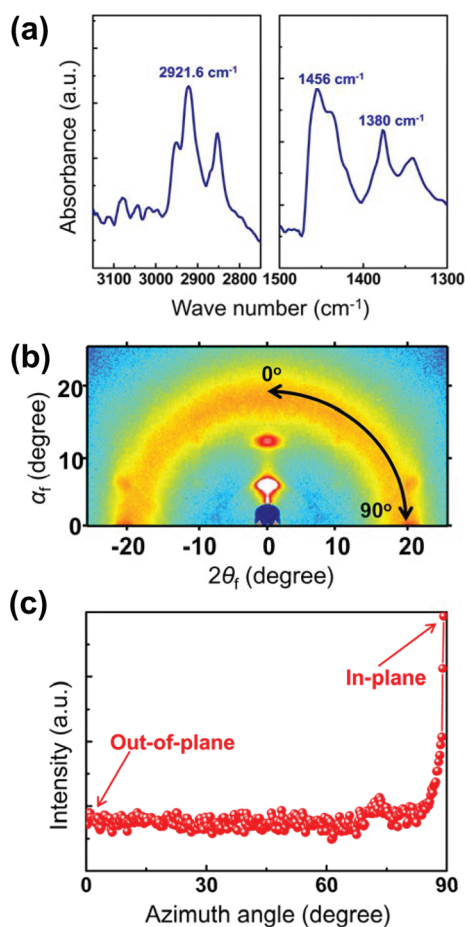


**Figure 3.** (a) IR spectrum of the PDHTT film. (b) 2D GIXS scattering pattern and (c) intensity profile along the azimuth angle scanned at  $19^\circ$ .

The value of  $\mu$  was extracted in the saturation regime for each OTFT from the slope of the square root of the drain current versus the gate voltage and found to be as high as  $0.003\text{ cm}^2\text{ V}^{-1}\text{ s}^{-1}$  (average,  $0.001\text{ cm}^2\text{ V}^{-1}\text{ s}^{-1}$ ), and the devices were found to exhibit on/off current ratios of up to  $10^5$  (Figure 4b). This low value of  $\mu$  might be due to the low molecular weight

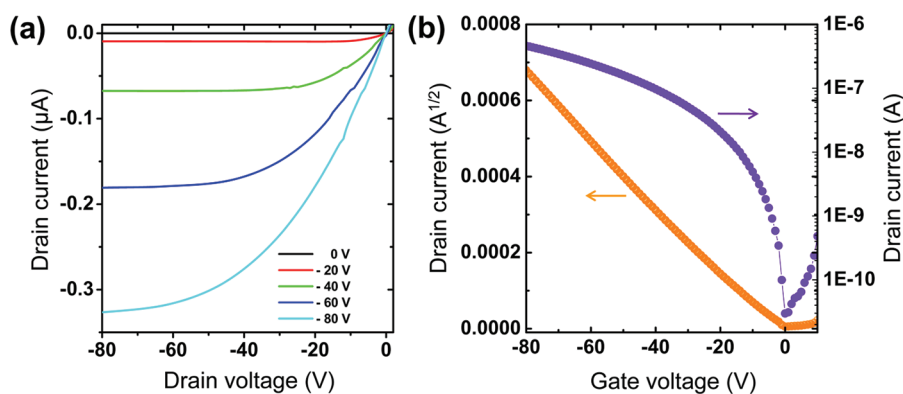


**Figure 4.** (a)  $I_D$ – $V_D$  output characteristics of the PDHTT-based OTFTs and (b) the  $I_D$ – $V_G$  transfer characteristics in the saturation regime ( $V_D = -80$  V).

( $M_n = 3.2 \text{ kgmol}^{-1}$ ) of the polymer and the wide  $\pi$ – $\pi$  stacking distance (4.2 Å). However, the transfer characteristics indicate good operation with a near-zero turn-on voltage, a small threshold voltage of  $-6.8$  V, and a subthreshold slope of  $\sim 1.8 \text{ Vdecade}^{-1}$ . More importantly, almost no hysteresis and bias stress effects were observed in these devices (see the Supporting Information S3).

We conducted a stability test to evaluate the lifetimes of the PDHTT OTFTs under a relative humidity of  $70 \pm 10\%$  in a thermo-hygrostat at a constant temperature of  $25$  °C, in darkness. The device was found to exhibit excellent air stability, maintaining a nearly constant value of  $\mu$  for 50 days after first 3 days and a good stability against humidity that is significantly

gate-independent values of  $\mu$  and the subthreshold swing (see the Supporting Information S4), which is probably due to the narrow trap distribution of the polymer films caused by the development of well-packed crystalline structures of PDHTT.

The transistors based on PDHTT show good temperature stability. In a thermogravimeter measurement, the  $T_d$  of PDHTT was found to be  $409$  °C under  $N_2$  (Supporting Information S5a). In a differential scanning calorimetry test, the trace of PDHTT was featureless up to  $400$  °C under  $N_2$  (Supporting Information S5b). In addition, in situ GIXS (Figure 6a) and AFM (Figure 1b–f) analyses showed that there are no significant alterations in the microstructures and morphologies of PDHTT films exposed to high temperatures; these results imply good temperature stability and the absence of structural transitions. The value of  $\mu$  for the PDHTT OTFTs was maintained up to  $250$  °C, in sharp contrast to the drastic degradation in the value of  $\mu$  degradation of an rr-P3HT device under identical conditions (Figure 6b).<sup>18</sup>

In general, the stability of conjugated semiconductors in air can be improved by deepening the HOMO level;<sup>13,14</sup> in the case of PDHTT, the distorted planarity along the backbone causes the conjugation length to be shorter, which gives greater air stability. Further, the backbone of PDHTT is not oxidized even at  $250$  °C; this result cannot be explained in terms of the HOMO level (5.1 eV) alone because some semiconductors with low HOMO levels exhibit poor air stability.<sup>15,16</sup> A close-packed frustrated structure with improved crystallinity results in superior air stability due to the increases in the packing density.<sup>17</sup> Similarly, OSCs with substantial interdigitation possess three-dimensional stacking with enlarged lateral ordering.<sup>11</sup> PDHTT also exhibits an interdigitated crystalline structure even among the very short hexyl side chains.<sup>21</sup> The highly stacked interdigitated crystalline structure of PDHTT results in thermal and air stability due to the resulting blocking of the penetration of  $O_2$  and  $H_2O$ .

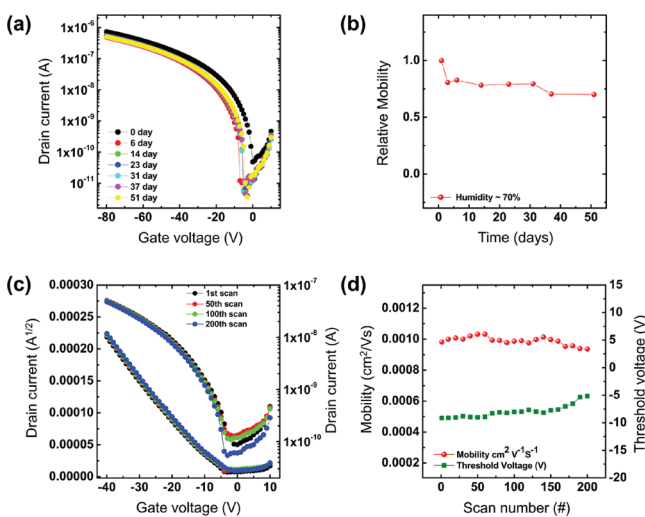


**Figure 5.** Humidity–exposure measurements for a PDHTT-based OTFT for 50 days: variations in (a) the transfer curve and (b) the field-effect mobility. Electrical characteristics of PDHTT-based OTFTs after repeated operation 200 times in air: (c) transfer curves and (d) field-effect mobilities and the threshold voltage.

better than those of rr-P3HT, PQT-12, and PBTTT (Figure 5a, b).<sup>4–6</sup>

The PDHTT OTFTs were also found to be electrically stable during device operation (Figure 5c–d): the values of  $\mu$  were determined during repeated stressing, where  $V_D$  was  $-40$  V and  $V_G$  was swept back and forth repeatedly between  $20$  and  $-40$  V. The devices were found to exhibit remarkable electrical stability during 200 successive operations in air. The devices also exhibit

## CONCLUSION

We have synthesized a novel polymer, poly(3,6-dihexyl-[2,2']bi[thieno[3,2-b]thiophene]) (PDHTT), which has a low HOMO level (5.1 eV) and an interdigitated lamellar structure. PDHTT-based OTFTs exhibit stable performance in a 70% humidity environment for 50 days and good electrical stability under repeated operation. Moreover, PDHTT does not degrade at temperatures up to  $250$  °C. We have demonstrated that the low HOMO level and the interdigitated crystalline structure of PDHTT result in its superior stability. These

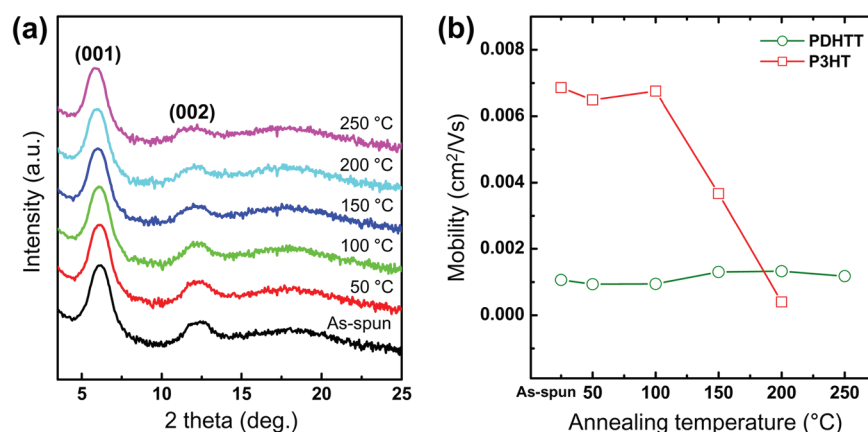


**Figure 6.** (a) In situ GIXS patterns of PDHTT films annealed at various temperatures and (b) field-effect mobilities of PDHTT and P3HT OTFTs annealed at various temperatures.

results show that PDHTT is a good candidate polymeric semiconductor for next-generation flexible electronics.

## ■ ASSOCIATED CONTENT

### Supporting Information

NMR data, cyclic voltammetry result, UV–vis absorption spectra, TGA and DSC thermal analyses, and hysteresis behavior of PDHTT OTFTs are included. This material is available free of charge via the Internet at <http://pubs.acs.org/>.

## ■ AUTHOR INFORMATION

### Corresponding Author

\*Tel: +82-54-279-2269 (C.E.P.); +82-41-860-1337 (J.K.), +82-54-279-2120 (M.R.). Fax: +82-54-279-8298 (C.E.P.); +82-41-867-5396 (J.K.); +82-54-279-3399 (M.R.). E-mail: cep@postech.edu (C.E.P.); jko@korea.ac.kr (J.K.); ree@postech.edu (M.R.).

## ■ ACKNOWLEDGMENTS

This study was supported by Grant 2010000809 from the Korea Science and Engineering Foundation (KOSEF) funded by the Korea government (NEST), by Grant R31-2008-000-10035-0 from the WCU program, and by the NRF of Korea (Grant 20090079630 and Center for EPB in Adv. Mater. Systems) and MEST (BK21 and WCU Programs).

## ■ REFERENCES

- (1) Sirringhaus, H.; Brown, P. J.; Friend, R. H.; Nielsen, M. M.; Bechgaard, K.; Langeveld-Voss, B. M. W.; Spiering, A. J. H.; Janssen, R. A. J.; Meijer, E. W.; Herwig, P.; De Leeuw, D. M. *Nat. Mater.* **1999**, *401*, 685.
- (2) Muccini, M. *Nat. Mater.* **2006**, *5*, 605.
- (3) Tsao, H. N.; Cho, D.; Andreasen, J. W.; Rouhanipour, A.; Breiby, D. W.; Pisula, W.; Mullen, K. *Adv. Mater.* **2009**, *21*, 209.
- (4) Majewski, L. A.; Kingsley, J. W.; Balocco, C.; Song, A. M. *Appl. Phys. Lett.* **2006**, *88*, 222108.
- (5) Ong, B. S.; Wu, Y.; Liu, P.; Gardner, S. J. *Am. Chem. Soc.* **2004**, *126*, 3378.
- (6) McCulloch, I.; Heeney, M.; Bailey, C.; Genevicius, K.; Macdonald, I.; Shkunov, M.; Sparrowe, D.; Tierney, S.; Wagner, R.; Zhang, W.; Chabiny, M. L.; Kline, R. J.; McGehee, M. D.; Toney, M. F. *Nat. Mater.* **2006**, *5*, 328.
- (7) Wu, Y.; Liu, P.; Ong, B. S.; Srikumar, T.; Zhao, N.; Botton, G.; Zhu, S. *Appl. Phys. Lett.* **2005**, *86*, 142102.

- (8) Sirringhaus, H.; Wilson, R. J.; Friend, R. H.; Inbasekaran, M.; Wu, W.; Woo, E. P.; Grell, M.; Bradley, D. D. C. *Appl. Phys. Lett.* **2000**, *77*, 406.
- (9) Salleo, A.; Street, R. A. *J. Appl. Phys.* **2003**, *94*, 471.
- (10) Kline, R. J.; DeLongchamp, D. M.; Fischer, D. A.; Lin, E. K.; Richter, L. J.; Chabiny, M. L.; Toney, M. F.; Heeney, M.; McCulloch, I. *Macromolecules.* **2007**, *40*, 7960.
- (11) Philippe, L.; Raimundo, J.-M.; Turbiez, M.; Monroche, V.; Allain, M.; Sauvage, F.-X.; Roncali, J.; Frere, P.; Skabara, P. J. *J. Mater. Chem.* **2003**, *13*, 1324.
- (12) He, M.; Zhang, F. *J. Org. Chem.* **2007**, *72*, 442.
- (13) Liu, J.; Zhang, R.; Osaka, I.; Mishra, S.; Javier, A. E.; Smilgies, D.-M.; Kowalewski, T.; McCullough, R. D. *Adv. Funct. Mater.* **2009**, *19*, 3427.
- (14) Cho, S.; Seo, J. H.; Park, S. H.; Beaupre, S.; Leclerc, M.; Heeger, A. J. *Adv. Mater.* **2010**, *22*, 1253.
- (15) Murphy, A. R.; Liu, J.; Luscombe, C.; Kavulak, D.; Frechet, J. M. J.; Kline, R. J.; McGehee, M. D. *Chem. Mater.* **2005**, *17*, 4892.
- (16) Kong, H.; Chung, D. S.; Kang, I.-N.; Lim, E.; Jung, Y. K.; Park, J.-H.; Park, C. E.; Shim, H.-K. *Bull. Korean Chem. Soc.* **2007**, *28*, 11.
- (17) Chung, D. S.; Park, J. W.; Kim, S.-O.; Heo, K.; Park, C. E.; Ree, M.; Kim, Y.-H.; Kwon, S.-K. *Chem. Mater.* **2009**, *21*, 5499.
- (18) Mattis, B. A.; Chang, P. C.; Subramanian, V. *Mater. Res. Soc. Symp. Proc.* **2003**, *71*, L10.35.1.
- (19) Moon, I. K.; Kim, N. *Dyes. Pigments.* **2008**, *78*, 207.
- (20) Sato, M.; Asami, A.; Maruyama, G.; Kosuge, M.; Nakayama, J.; Kumakura, S.; Fujihara, T.; Unoura, K. *J. Organomet. Chem.* **2002**, *56*, 654.
- (21) Northrip, J. E.; Chabiny, K. L.; Hamilton, R.; McCulloch, I.; Heeney, M. *J. Appl. Phys.* **2008**, *104*, 083705.
- (22) Miguel, L. S.; Matzger, A. J. *Macromolecules.* **2007**, *40*, 9233.
- (23) McCulloch, I.; Heeney, M.; Chabiny, M. L.; DeLongchamp, D.; Kline, R. J.; Colle, M.; Duffy, W.; Fisher, D.; Gundlach, D.; Hamadani, B.; Hamilton, R.; Richter, L.; Salleo, A.; Shkunov, M.; Sparrowe, D.; Tierney, S.; Zhang, W. *Adv. Mater.* **2009**, *21*, 1091.
- (24) John, C. *Encyclopedia of Analytical Chemistry*; Wiley: New York, 2000; p 10815